Contact Doping as a Design Strategy for Compact TFT-Based Temperature Sensing

Eva Bestelink, *Graduate Student Member, IEEE*, Hao-Jing Teng, and Radu A. Sporea, *Senior Member, IEEE*

***Abstract*— Contact-controlled devices, such as source-gated transistors (SGTs), deliberately use energy barriers at the source, and naturally, the positive temperature dependence (PTD) of drain current can be utilized for temperature sensing. We exploit the difference in drain current activation energy, which arises with contact doping in polysilicon n-type contact-controlled transistors, to demonstrate output current with either a PTD or negative temperature dependence (NTD). The range over which output current varies linearly with temperature, as well as the sensitivity, can be tailored by the choice of reference current magnitude and relative source contact properties within the current mirror. The sensing scheme simplifies the circuit design because it relies solely on thin-film transistors and it has inherent immunity to output voltage variation. This ability to tune the sign of temperature dependence allows facile integration in applications requiring homeostasis via feedback, e.g., electronic skin, in a minimal layout area and potentially with convenient reduction of patterning steps during fabrication.**

***Index Terms*— Activation energy, analog circuits, Schottky barrier, temperature dependence, temperature sensor, thin-film transistor (TFT).**

I. Introduction

EMERGING flexible electronics, such as smart skin [1] or multimodal sensing [2], typically integrate a temperature sensing element, e.g., thermistor, with circuits comprising thin-film transistors (TFTs) [3]. In some cases, functional materials are incorporated in the TFT architecture itself, e.g., pyroelectric gate insulator [4].

While such sensors require uniform and reliable performance [2], the same is required of any adjunct circuit comprising TFTs [5], which have to withstand the challenges of low-cost manufacturing to become commercially viable [6]. Contact-controlled TFTs, such as source-gated transistors (SGTs) [7]–[10], on the other hand, have many features that allow it to stand out as a candidate device for developing compact sensing circuits. Some of its benefits include tolerance to bias and mechanical stress [11]–[13], high gain with absence of kink effect [8], and, crucially, uniformity of operation with respect to material defects [14] and imprecise manufacturing processes [12]. Hence, SGTs, and related contact-controlled devices [15], would be highly suited to emerging flexible and/or disposable sensing technologies.

By engineering energy barriers at the source contact, SGTs, and other TFTs that comprise source energy barriers [15]–[19], naturally can be used to sense temperature [19]–[21], due to the positive temperature dependence (PTD) of drain current. However, linearity and sensitivity of the output current can be enhanced by exploiting contact-controlled architectures with different temperature dependencies [22]. SGTs [Fig. 1(a) and (b)], for example, either have a small or large PTD resulting from the dominant charge injection process [23], [24]. Consequently, SGT current mirrors can be designed to not only provide PTD but also to deliver an output current with negative temperature dependence (NTD) [22]. NTD functionality is usually obtained through a change in resistance of negative temperature coefficient thermistors and has various uses in sensing [25], [26]. However, like many other devices in thin-film fabrication, difficulties with integration restrict many “real product” applications [2].

We have previously shown how PTD and NTD can be generated by SGT current mirrors with differing source–gate overlap, S [22]. Here, we show an alternative method for creating devices with different activation energies and, hence, distinct behavior of the drain current with temperature. We demonstrate how these functional characteristics contribute to obtaining PTD or NTD in compact two-transistor temperature sensing circuits.

II. Experimental Methods

Low-temperature polysilicon (LTPS) SGTs [Fig. 1(a) and (b)] were fabricated in a self-aligned, bottom gate, top contact process. Cr was used to realize a Schottky barrier, with a 5-keV BF_2 implant to modify the height of the energy barrier, in the source window, before deposition of the contact metal [Fig. 1(a)]. Here, a concentration of 1×10^{13} cm^{-2} and 7.5×10^{13} cm^{-2} was used to further raise the contact barrier, creating devices that will be referred to as low and high contact doping, respectively. The drain region was made Ohmic with a high P implant. Device geometry is identical to ensure that temperature behavior is solely attributed to the contact doping and includes: 200 nm of SiN_x and 200-nm SiO_2 gate insulator, 40-nm LTPS, width $= 50$ μm, source–gate overlap $S = 2$ μm, and source–drain separation $d = 6$ μm (see [27] for full process details).

Devices and circuits were measured with a Keysight B2902A source/measure unit (SMU) connected to a Wentworth probe station with a temperature-controlled chuck.

Manuscript received June 22, 2021; revised August 11, 2021; accepted August 17, 2021. Date of publication August 27, 2021; date of current version September 22, 2021. This work was supported by Engineering and Physical Sciences Research Council (EPSRC) under Grant EP/R028559/1 and Grant EP/V002759/1. The review of this article was arranged by Editor J.-S. Park. *(Corresponding author: Radu A. Sporea.)*

The authors are with the Advanced Technology Institute, Department of Electrical and Electronic Engineering, University of Surrey, Guildford GU2 7XH, U.K. (e-mail: r.a.sporea@surrey.ac.uk).

Color versions of one or more figures in this article are available at https://doi.org/10.1109/TED.2021.3106276.

Digital Object Identifier 10.1109/TED.2021.3106276

This work is licensed under a Creative Commons Attribution 4.0 License. For more information, see https://creativecommons.org/licenses/by/4.0/

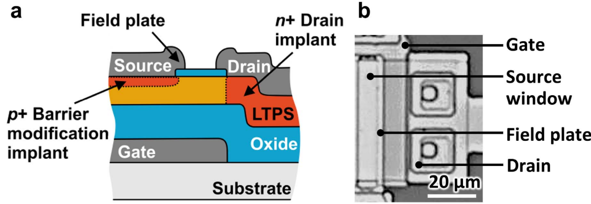

Fig. 1. (a) Cross section schematic of a self-aligned LTPS SGT with BF_2 barrier modification implant at the source contact. (b) Photomicrograph of a typical LTPS SGT.

Current mirrors were created by using a six-probe setup, with either the device with high or low contact doping as the input transistor. Reference currents of $I_{ref} = 2$, 3, and 4 μA were applied to the input transistor via the SMU for temperature sensing measurements.

III. Results and Discussion

A. SGT Characterization

A comparison of output characteristics [Fig. 2(a) and (b)] for two identical LTPS SGTs, which only differ in source contact doping, shows, as expected, that a lower contact doping concentration results in higher drain current. Both devices show saturation characteristics indicative of source pinchoff by their very low saturation and minimal dependence on drain voltage V_D [8], [27].

These output curves are characteristic of contact-controlled transistors and are advantageous for energy-efficient circuit operation. The early saturation behavior of SGTs would be particularly beneficial for applications where supply voltages are limited, e.g., the Internet of Things (IoT) devices.

The transfer characteristics in Fig. 2(c) shows that the transistor with the high contact doping has, in fact, a lower temperature dependence of drain current. This is verified by the activation energy plot in Fig. 2(d) and warrants a separate investigation. The effect could be attributed to interfacial damage, partial dopant activation, or influence of minority carriers due to significant band bending.

The dissimilar activation energies for charge injection at the source electrode [Fig. 2(d)] result in saturated drain currents with positive, but different, variations with temperature. Due to the high output impedance of SGTs, drain current does not vary significantly with V_D across the temperature range. Here, activation energy was initially measured at $V_D = 5$ V and, 183 days later, at $V_D = 3$ and 10 V. The behavior is practically identical with only small variations in chuck temperature contributing to the discrepancies.

B. Temperature Sensing With SGT Current Mirrors

When transistors are used in current mirrors, the gate-to-drain connection of the input transistor imposes a minimum current limit for correct current copying (i.e., $V_G = V_D$ cannot be negative). Enhancement mode operation would be preferred, and however, the depletion-mode devices used here to demonstrate the general operating principle.

Current copying performance is shown in Fig. 3(a) and (b) for current mirrors in which the input transistor [M1, see inset of Fig. 3(b)] is chosen as either the device with high or low contact doping. Previously, we have shown that current mirrors using identical SGTs have exceptional current copying performance and show no temperature dependence [22].

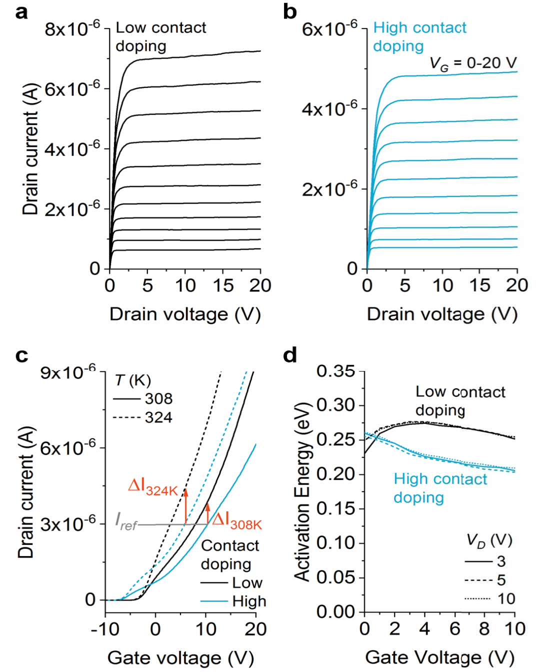

Fig. 2. Output characteristics for SGTs with BF_2 implant of (a) 1×10^{13} cm^{-2} (low doping) and (b) 7.5×10^{13} cm^{-2} (high doping). Both devices share the same geometry with source–gate overlap $S = 2$ μm. $V_G = 0$–20 V, step 2 V. (c) Transfer characteristics of the devices showing the difference in drain current ΔI for two temperatures T when the transistors are connected in a current mirror configuration with a reference current $I_{ref} = 3$ μA. (d) Activation energy in saturation showing the device with the higher contact doping has a lower activation energy. Measurements for $V_D = 3$ and 10 V were taken 183 days after $V_D = 5$ V, demonstrating long-term repeatability. In the expected operating regime in the current mirror configuration, V_G decreases with temperature and does not exceed 10 V for $I_{ref} = 3$ μA.

For temperature sensing, we can exploit differences in temperature behavior of each device to provide output current with PTD [Fig. 3(a)] or NTD [Fig. 3(b)].

This effect correlates to the previously shown operation of circuits implemented with SGTs in which the mismatched temperature dependence is realized by varying source–gate overlap S [22]. The approach shown here can be implemented with devices of minimal feature size and may be advantageous in cases where area is limited. In such cases, tuning of barrier properties would be a preferred route (e.g., pixels in high-resolution sensing arrays). One possible application with strict areal requirements would be display and signage, as in-pixel temperature sensing is a desirable feature [28] and autonomous compensation exploiting NTD might be of value.

To obtain a PTD, the device with the lower activation energy should receive I_{ref} (M1). As temperature increases, the two SGT's V_G decreases to maintain I_{ref} flowing through M1, but M2's higher activation energy results in a net increase of its drain current, even as V_G reduces [Fig. 3(c)]. From the measurements, the temperature sensitivity of output current (TSOC) was calculated at +1.19, +1.18, and +0.82%K^{-1} for 2, 3, and 4 μA, respectively, for this combination. The results in Fig. 3(c) indicate that the optimum range for sensing (where the curve is linear) can be tuned for low or high temperatures by driving M1 with lower or higher I_{ref}, respectively. The range over which linear response to temperature is achieved is bound by the operating conditions of M1 and

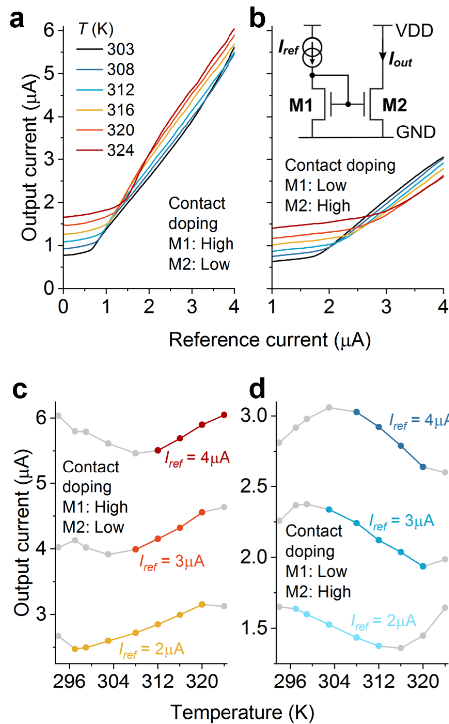

Fig. 3. Current mirror output current dependence on reference current with (a) high-to-low and (b) low-to-high contact doping of SGTs as M1 and M2, respectively, in the circuit (inset). Depending on the current mirror configuration, output current with (c) PTD or (d) NTD can be generated. In both PTD and NTD current mirrors, the sensing range, as well as the resolution, can be tuned via I_{ref}.

M2. Specifically, both devices are required to be working in saturation (which translates to a minimum gate voltage, and implicitly drain current, for the diode-connected transistor M1) and above threshold (to ensure that the drain current is determined by the pinched-off area at the source). It should be noted that, since the gate voltage of M2 decreases with temperature in this configuration, the output current will have a lower temperature dependence than if M2 were to be operating at a constant gate voltage, e.g., $V_{\text{GS}} = 0$ V for this depletion-mode device.

The versatility of the schematic manifests in the ability to produce NTD with unipolar devices. To achieve NTD, the two transistors are swapped. M1 now has the higher activation energy, requiring a relatively large reduction of V_{G} with temperature to keep its drain current constant. M2 now has a comparatively lower temperature dependence, so its increase of drain current with temperature cannot compensate for the reduction in its gate voltage, thereby creating a negative temperature coefficient of output current [Fig. 3(d)] with a TSOC of −1.06, −1.01, and $-1.07\%\text{K}^{-1}$ for $I_{\text{ref}} = 2$, 3, and 4 μA, respectively. Again, a higher I_{ref} translates the range of linearity toward higher temperatures.

For PTD, output current changes by 17, 20, and 33 nAK^{-1} for $I_{\text{ref}} = 2$, 3, and 4 μA, respectively, whereas NTD demonstrates a higher resolution of 30, 48, and 45 nAK^{-1}. This increased sensitivity for NTD is a consequence of device operation. For the same geometry and gate bias, high and low activation energy devices have different drain currents. This leads to distinct absolute changes, while relative variations with temperature are similar.

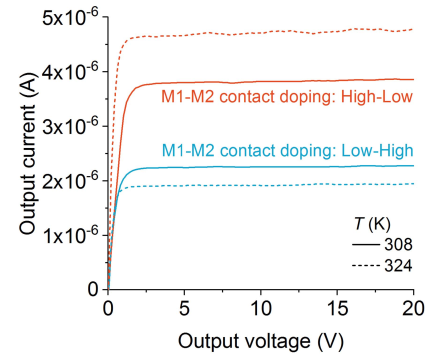

Fig. 4. Output current for $I_{\text{ref}} = 3$ μA is largely independent of output voltage, an advantageous feature that SGTs possess over other Schottky barrier TFTs. Designing such devices to operate in enhancement mode would allow for lower gate voltage operation (<3 V), suitable for energy-constrained IoT applications.

As the required bias voltage is lower for reduced I_{ref}, the circuits are capable of operating below $V_{\text{G}} = 5$ V, in a temperature range suitable for human body temperature sensing, among other applications in which the range of interest is relatively constrained. For example, NTD with $I_{\text{ref}} = 2$ μA requires $V_{\text{G}} = 4.12$ V at $T = 308$ K and reduces to 2.99 V at 312 K. In addition, the SGT's robust performance under bias stress [20] would allow for continuous temperature monitoring and feedback.

Finally, both PTD and NTD circuits provide output currents that do not vary with supply or load voltage, due to the high output impedance of SGTs (Fig. 4). It is likely that conventional TFT implementations would require cascoding and higher operating voltages to offer comparable power supply regulation. In principle, designing these SGTs to operate with a low positive threshold voltage would lead to low supply voltage operation (e.g., $V_{\text{DD}} < 3$ V), an attractive proposition for sensing circuits in distributed or autonomous IoT applications.

The principles outlined here translate to other contact-controlled devices [15], as well as to different means of barrier engineering in diverse materials [17]–[19], [29], with applications in unsupervised temperature-dependent control, such as homeostasis. Here, the ability to produce an output current that decreases with temperature would lead to smart systems beyond display technology [28]. For example, smart therapeutic systems [30]–[32] integrated into wound dressings to maintain an optimum healing environment [33].

The circuit presented here is optimized for human core temperature measurement. However, contact doping, geometry, and reference current are design parameters with which to tune the temperature range of interest as well as resolution. Hence, these compact circuits capable of both PTD and NTD output, and realized with unipolar devices for low-cost manufacturing, would benefit highly functional autonomous temperature sensing systems, particularly for healthcare solutions.

While the use of doping to modify source contact activation energy is effective, consideration needs to be given to process cost and complexity. To simplify implementation, a process may be chosen in which one of the two transistors within the mirror circuit has an undoped rectifying contact. In this case, several processing steps may be combined, for example, field-relief structures definition and contact doping through the same contact window in top-contact LTPS SGTs [34].

IV. Conclusion

We have demonstrated a compact implementation of versatile temperature sensing circuits based on unipolar polysilicon TFTs. In this realization, the temperature dependence is achieved by using SGTs of identical geometry but with different charge injection activation energies.

This method complements our previous solution in which the source injection area was altered to create devices with different temperature behaviors. Changing relative device geometry is likely to be preferred in most implementations, due to reduced processing steps. However, tuning the respective source contact properties of transistors with minimal feature size may find uses in arrays where area reduction is a strict priority.

Acknowledgment

The authors would like to thank J. M. Shannon for his advice.

References

[1] K. J. Yu, Z. Yan, M. Han, and J. A. Rogers, "Inorganic semiconducting materials for flexible and stretchable electronics," *NPJ Flexible Electron.*, vol. 1, no. 1, pp. 1–13, Sep. 2017, doi: 10.1038/s41528-017-0003-z.

[2] S. Jeon, S.-C. Lim, T. Q. Trung, M. Jung, and N.-E. Lee, "Flexible multimodal sensors for electronic skin: Principle, materials, device, array architecture, and data acquisition method," *Proc. IEEE*, vol. 107, no. 10, pp. 2065–2083, Oct. 2019, doi: 10.1109/JPROC.2019.2930808.

[3] X. Ren *et al.*, "A low-operating-power and flexible active-matrix organic-transistor temperature-sensor array," *Adv. Mater.*, vol. 28, no. 24, pp. 4832–4838, Apr. 2016, doi: 10.1002/adma.201600040.

[4] N. T. Tien, Y. G. Seol, L. H. A. Dao, H. Y. Noh, and N.-E. Lee, "Utilizing highly crystalline pyroelectric material as functional gate dielectric in organic thin-film transistors," *Adv. Mater.*, vol. 21, pp. 910–915, Feb. 2009, doi: 10.1002/adma.200801831.

[5] A. Nathan *et al.*, "Flexible electronics: The next ubiquitous platform," *Proc. IEEE*, vol. 100, pp. 1486–1517, May 2012, doi: 10.1109/JPROC.2012.2190168.

[6] A. F. Paterson and T. D. Anthopoulos, "Enabling thin-film transistor technologies and the device metrics that matter," *Nature Commun.*, vol. 9, no. 1, pp. 1–4, Dec. 2018, doi: 10.1038/s41467-018-07424-2.

[7] J. M. Shannon and E. G. Gerstner, "Source-gated thin-film transistors," *IEEE Electron Device Lett.*, vol. 24, no. 6, pp. 405–407, Jun. 2003, doi: 10.1109/LED.2003.813379.

[8] R. A. Sporea, M. J. Trainor, N. D. Young, J. M. Shannon, and S. R. P. Silva, "Source-gated transistors for order-of-magnitude performance improvements in thin-film digital circuits," *Sci. Rep.*, vol. 4, no. 1, pp. 1–7, May 2015, doi: 10.1038/srep04295.

[9] J. Zhang *et al.*, "Extremely high-gain source-gated transistors," *Proc. Nat. Acad. Sci. USA*, vol. 116, no. 11, pp. 4843–4848, Mar. 2019, doi: 10.1073/pnas.1820756116.

[10] A. S. Dahiya *et al.*, "Temperature dependence of charge transport in zinc oxide nanosheet source-gated transistors," *Thin Solid Films*, vol. 617, pp. 114–119, Oct. 2016, doi: 10.1016/j.tsf.2016.02.021.

[11] R. A. Sporea, X. Guo, J. M. Shannon, and S. R. Silva, "Source-gated transistors for versatile large area electronic circuit design and fabrication," *ECS Trans.*, vol. 37, no. 1, pp. 57–63, Dec. 2019, doi: 10.1149/1.3600724.

[12] R. A. Sporea, A. S. Alshammari, S. Georgakopoulos, J. Underwood, M. Shkunov, and S. R. P. Silva, "Micron-scale inkjet-assisted digital lithography for large-area flexible electronics," in *Proc. Eur. Solid-State Device Res. Conf.*, Sep. 2013, pp. 280–283, doi: 10.1109/ESSDERC.2013.6818873.

[13] A. S. Dahiya *et al.*, "Single-crystalline ZnO sheet source-gated transistors," *Sci. Rep.*, vol. 6, no. 1, pp. 2–11, May 2016, doi: 10.1038/srep19232.

[14] R. A. Sporea, L. J. Wheeler, V. Stolojan, and S. R. P. Silva, "Towards manufacturing high uniformity polysilicon circuits through TFT contact barrier engineering," *Sci. Rep.*, vol. 8, no. 1, pp. 1–8, Dec. 2018, doi: 10.1038/s41598-018-35577-z.

[15] E. Bestelink, O. de Sagazan, L. Motte, B. Schultes, S. R. P. Silva, and R. A. Sporea, "Versatile thin-film transistor with independent control of charge injection and transport for mixed signal and analog computation," *Adv. Intell. Syst.*, vol. 3, no. 1, Jan. 2020, Art. no. 2000199, doi: 10.1002/aisy.202000199.

[16] C. Liu *et al.*, "A general approach to probe dynamic operation and carrier mobility in field-effect transistors with nonuniform accumulation," *Adv. Funct. Mater.*, vol. 29, no. 29, pp. 1–10, May 2019, doi: 10.1002/adfm.201901700.

[17] L. Wang, Y. Sun, X. Zhang, L. Zhang, S. Zhang, and M. Chan, "Tunneling contact IGZO TFTs with reduced saturation voltages," *Appl. Phys. Lett.*, vol. 110, no. 15, Apr. 2017, Art. no. 152105, doi: 10.1063/1.4980131.

[18] X. Wu *et al.*, "Improving ideality of P-type organic field-effect transistors via preventing undesired minority carrier injection," *Adv. Funct. Mater.*, vol. 31, no. 19, Feb. 2021, Art. no. 2100202, doi: 10.1002/adfm.202100202.

[19] S. Choi *et al.*, "Oxygen content and bias influence on amorphous InGaZnO TFT-based temperature sensor performance," *IEEE Electron Device Lett.*, vol. 40, no. 10, pp. 1666–1669, Oct. 2019, doi: 10.1109/LED.2019.2937157.

[20] R. A. Sporea, J. M. Shannon, and S. R. P. Silva, "High-resolution temperature sensing with source-gated transistors," in *Proc. 69th Device Research Conf.*, Sep. 2011, pp. 61–62, doi: 10.1109/DRC.2011.5994463.

[21] C. Zhu *et al.*, "Stretchable temperature-sensing circuits with strain suppression based on carbon nanotube transistors," *Nature Electron.*, vol. 1, no. 3, pp. 183–190, Mar. 2018, doi: 10.1038/s41928-018-0041-0.

[22] E. Bestelink *et al.*, "Compact source-gated transistor analog circuits for ubiquitous sensors," *IEEE Sensors J.*, vol. 20, no. 24, pp. 1–11, Jul. 2020, doi: 10.1109/JSEN.2020.3012413.

[23] R. A. Sporea, M. Overy, J. M. Shannon, and S. R. P. Silva, "Temperature dependence of the current in Schottky-barrier source-gated transistors," *J. Appl. Phys.*, vol. 117, no. 18, pp. 1–7, May 2015, doi: 10.1063/1.4921114.

[24] R. A. Sporea and S. R. P. Silva, "Design considerations for the source region of Schottky-barrier source-gated transistors," in *Proc. Int. Semiconductor Conf.*, Nov. 2017, pp. 155–158, doi: 10.1109/SMICND.2017.8101185.

[25] E. Flores-Martinez, M. J. Malin, J. Radtke, and L. A. DeWerd, "Challenges and opportunities in calorimetry for clinical radiation dosimetry," *AIP Conf. Proc.*, vol. 1747, Jun. 2016, Art. no. 110001, doi: 10.1063/1.4954145.

[26] D. Katerinopoulou *et al.*, "Large-area all-printed temperature sensing surfaces using novel composite thermistor materials," *Adv. Electron. Mater.*, vol. 5, no. 2, pp. 1–7, Dec. 2019, doi: 10.1002/aelm.201800605.

[27] R. A. Sporea, M. J. Trainor, N. D. Young, J. M. Shannon, and S. R. P. Silva, "Intrinsic gain in self-aligned polysilicon source-gated transistors," *IEEE Trans. Electron Devices*, vol. 57, no. 10, pp. 2434–2439, Aug. 2010, doi: 10.1109/TED.2010.2056151.

[28] Y. Chen, S. Lee, H. Kim, J. Lee, D. Geng, and J. Jang, "In-pixel temperature sensor for high-luminance active matrix micro-light-emitting diode display using low-temperature polycrystalline silicon and oxide thin-film-transistors," *J. Soc. Inf. Display*, vol. 28, no. 6, pp. 528–534, May 2020, doi: 10.1002/jsid.915.

[29] R. A. Sporea, K. M. Niang, A. J. Flewitt, and S. R. P. Silva, "Novel tunnel-contact-controlled IGZO thin-film transistors with high tolerance to geometrical variability," *Adv. Mater.*, vol. 31, no. 36, Jul. 2019, Art. no. 1902551, doi: 10.1002/adma.201902551.

[30] S. Schreml, R. M. Szeimies, L. Prantl, S. Karrer, M. Landthaler, and P. Babilas, "Oxygen in acute and chronic wound healing," *Brit. J. Dermatology*, vol. 163, no. 2, pp. 257–268, Apr. 2010, doi: 10.1111/j.1365-2133.2010.09804.x.

[31] Y. Liu, X. Zhao, C. Zhao, H. Zhang, and Y. Zhao, "Responsive porous microcarriers with controllable oxygen delivery for wound healing," *Small*, vol. 15, no. 21, pp. 1–7, Apr. 2019, doi: 10.1002/smll.201901254.

[32] J. I. Kang, K. M. Park, and K. D. Park, "Oxygen-generating alginate hydrogels as a bioactive acellular matrix for facilitating wound healing," *J. Ind. Eng. Chem.*, vol. 69, pp. 397–404, Jan. 2019, doi: 10.1016/j.jiec.2018.09.048.

[33] F. Strodtbeck, "Physiology of wound healing," *Newborn Infant Nursing Rev.*, vol. 1, no. 1, pp. 43–52, Mar. 2001, doi: 10.1053/nbin.2001.23176.

[34] R. A. Sporea, M. J. Trainor, N. D. Young, J. M. Shannon, and S. R. P. Silva, "Field plate optimization in low-power high-gain source-gated transistors," *IEEE Trans. Electron Devices*, vol. 59, no. 8, pp. 2180–2186, May 2012, doi: 10.1109/TED.2012.2198823.